Wideband and High-Gain Composite Cavity-Backed Crossed Triangular Bowtie Dipoles for Circularly Polarized Radiation

Shi-Wei Qu, Chi Hou Chan, *Fellow, IEEE*, and Quan Xue, *Senior Member, IEEE*

***Abstract*—A composite cavity-backed antenna excited by crossed triangular bowtie dipoles is proposed and investigated for circular polarization (CP) applications. It is fed by a novel balun, i.e., a transition from a microstrip line to double slot lines, providing symmetrical electric field distributions at the feeding port. Measurements of an optimized antenna prototype show that it can achieve an impedance bandwidth of over 57.6% for $\mathrm{SWR} \leq 2$, a 3-dB axial-ratio bandwidth of 39%, a broadside gain of $8-10.7$ dBi, and symmetrical radiation patterns over the whole operating band. The operating principles of the proposed antenna are analyzed carefully and found quite different from crossed thin-wire dipoles with very weak coupling. Problems in the feeding balun, greatly deteriorating the CP performance at the resonance, are clearly addressed and solved. Detailed parametric studies are given in the final part of this paper.**

***Index Terms*—Bowtie antennas, cavity-backed antennas, circular polarization, unidirectional patterns.**

I. Introduction

CIRCULARLY polarized (CP) antennas have been receiving much attention for the applications on wireless communications because they are not only able to reduce the multi-path effects but also to allow more flexible orientation of the transmitting and receiving antennas. Meanwhile, the unidirectional patterns are expected to provide high security and efficiency of the propagating channels in many cases.

A conventional method to construct an antenna with CP radiation is to produce two degenerate modes on the radiating element with one feeding point, such as single probe-fed, proximity-coupled and aperture-coupled CP patch antennas [1]–[3]. However, their axial-ratio (AR) bandwidths are always very small, generally a few percent which does not meet the bandwidth requirements in modern wideband communication systems. An improved method is to generate two orthogonal modes separately with dual- or multi-fed mechanism, such as patch antennas fed by L-probe and aperture coupling techniques [4], [5], and although the $\mathrm{AR} \leq 3$ dB bandwidth can be enhanced to over 40%, the complicated feeding networks are required and the broadside gains are generally below 8 dBi. Additionally, the sequential arrangement of linearly or circularly polarized antenna elements can also produce CP radiation in a large frequency band, but at the cost of large total dimensions [6], [7].

A straightforward way for CP radiation is to employ two orthogonally crossed dipoles fed by two sources with equal magnitude and 90° phase difference. However, the feeding network also complicates the antenna design and fabrication [8]–[11]. In 1961, it was reported that single-fed crossed dipoles connected in parallel could also generate CP radiation if the lengths of the dipoles were chosen such that the real parts of their input admittances are equal and the phase angles of their input admittances differ by 90°[12]. According to these conditions, several crossed-dipole antennas were developed. A short backfire antenna excited by two crossed slots can present a 4.2% AR bandwidth with a 14-dBi gain [13]. Also reported is a crossed-slot antenna, backed by a metal plate with a quarter wavelength height, which features a 5% AR bandwidth and a 10-dBi gain [14]. Another crossed-dipole antenna with a reactively loaded parasitic loop is developed for land mobile satellite communications [15]. However, all of these antennas show a small AR bandwidth, at most 15%, and are also unsuitable for modern wideband communication systems.

In our previous studies, a series of unidirectional cavity--backed bowtie antennas for wideband applications were developed [16]–[20], and the operating principles of this kind of antenna are essentially investigated based on previous outstanding contributions [21], and both their advantages and disadvantages are extensively discussed in these works. However, all of our previous works were focused on linearly polarized (LP) applications. In this paper, cavity-backed structures are also employed to construct a wideband CP antenna. The same composite cavity to [17] is utilized to optimize the electric field distributions for stable radiation patterns. A pair of crossed bowtie dipoles (CBD), formed by crossing two triangular bowtie dipoles together, is employed as the exciter which determines the operating frequency and final bandwidth to some extent. The sharp corners of larger triangular bowtie dipole are rounded based on our previous research [18] and the smaller one is loaded by two overlapped gaps, offering a flexible input capacitance within most part of the interesting

Manuscript received July 12, 2009; revised January 13, 2010; accepted April 03, 2010. Date of publication July 01, 2010; date of current version October 06, 2010. This work was supported by the Research Grants Council of Hong Kong SAR, China, under [Project No. CityU122407].

S.-W. Qu was with the State Key Laboratory of Millimeter Waves, City University of Hong Kong, Kowloon, Hong Kong, China. He is now with Tohoku University, Sendai, Japan (e-mail: dyon.qu@gmail.com).

C. H. Chan and Q. Xue are with the State Key Laboratory of Millimeter Waves, City University of Hong Kong, Kowloon, Hong Kong, China (e-mail: dyon.qu@gmail.com).

Color versions of one or more of the figures in this paper are available online at http://ieeexplore.ieee.org.

Digital Object Identifier 10.1109/TAP.2010.2055792

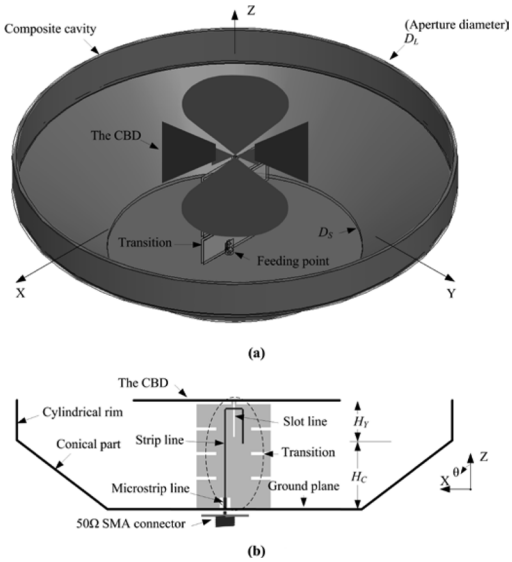

Fig. 1. Geometry of the proposed composite cavity-backed CBD.

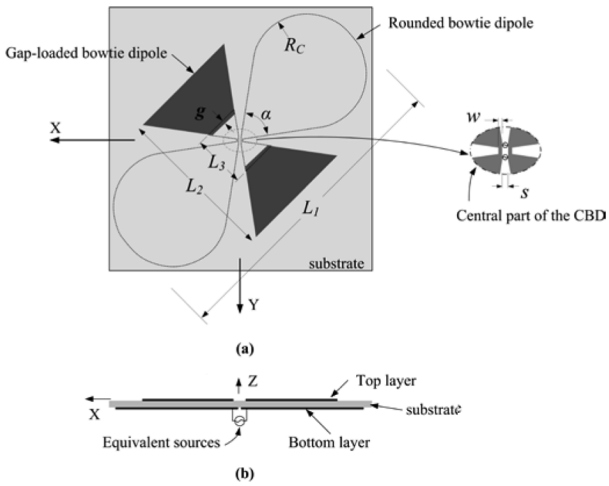

Fig. 2. Geometry of the CBD.

frequency band. Measured results of the fabricated antenna prototype verify simulations with reasonably good agreements.

II. Geometry of Composite Cavity-Backed CBD

Fig. 1 shows the geometry of the proposed antenna, consisting of a composite cavity, a CBD as an exciter, a transition from a microstrip line to double slot lines (DSL), and an SMA connector placed under the cavity to feed the antenna. The CBD is arranged similar to the exciter in [17] for the lowest profile. Fig. 2 shows the geometry of the CBD and its parameters in detail, and the deep color denotes its shape on the top side of the substrate and the dashed line shows that on the bottom side. The exciter consists of a larger triangular bowtie dipole with rounded corners and a smaller one with two overlapping parts between the top and the bottom layers, corresponding to capacitive loadings. The desired input reactance of smaller triangular bowtie dipole can be easily achieved by tuning L_3 and g, representing position and value of the capacitive loading, respectively. The smaller dipole is not rounded due to the reasons mentioned in the next section. The CBD is built on a substrate with thickness of

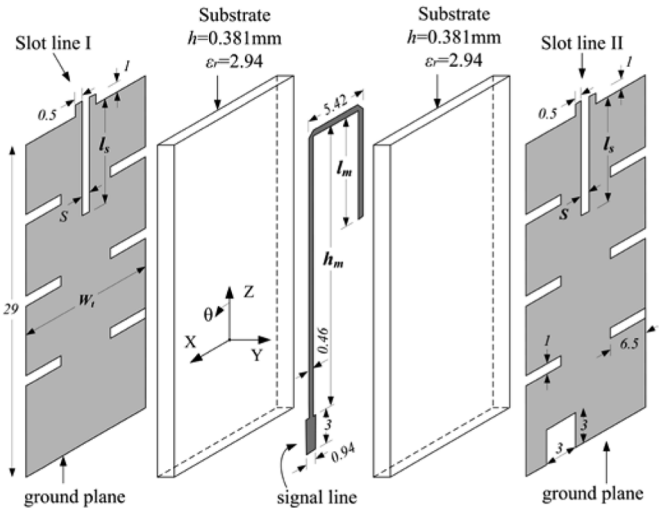

Fig. 3. Geometry of the transition from the microstrip line to double slot line (in mm).

0.5 mm and relative permittivity $\varepsilon_r = 2.65$ for easy fabrication and support. For clarity, the central part of the CBD is scaled and given as the inset in the right side of Fig. 2(a). For parallel connection of the two dipoles, a narrow strip with width w is utilized to connect one arm of the larger bowtie dipole and that of the smaller one, and a small gap of s is located at its vertexes for connection with the DSL of the transition. The geometry of the microstrip-to-DSL transition, with two dielectric and three metallic layers, is given in Fig. 3, and it is mounted vertically on the ground plane and fabricated on a substrate with $\varepsilon_r = 2.94$ and 0.381-mm thickness. The DSL section of the transition features a symmetrical structure along both XZ and YZ planes, so the transition can provide symmetrical electric field distributions on the DSL port, which can induce more balanced currents on the CBD than that used in [22]. Several pairs of slots cut on the ground of the transition are employed to lower the resonant frequency of the transition out of the 3-dB AR band, because the resonance of the transition would greatly deteriorate the CP performances at that frequency point, as given in Section III.

In the design procedure, the proposed antenna without the feeding transition is optimized firstly using the parameterized model within the HFSS [23], and then the transition is added for impedance matching considerations. The first step is the most critical and time-consuming one, while the impedance matching is much easier by just tuning l_s, l_m, and h_m. The required computer source may be interesting for antenna designer. As far as our computer is concerned, there are 3-GB memory, Intel Core 2 CPU @ 2.66 GHz, and 32-bit Windows XP Operating System, and each simulation will cost around 1.5-GB memory and 1-hour time (It will require larger memory and longer time for the whole antenna simulation after adding the transition), which is not an unacceptable configuration for modern personal computers.

The optimized geometrical parameters are given as follows (in mm): $D_S = 70$ ($0.6\lambda_0$, where λ_0 is the free-space wavelength at the center of the AR ≤ 3 dB frequency band), $D_L = 120$ ($1.028\lambda_0$, aperture diameter), $H_Y = 10$ ($0.086\lambda_0$, height of cylindrical part of the cavity), $H_C = 20$ ($0.171\lambda_0$, height

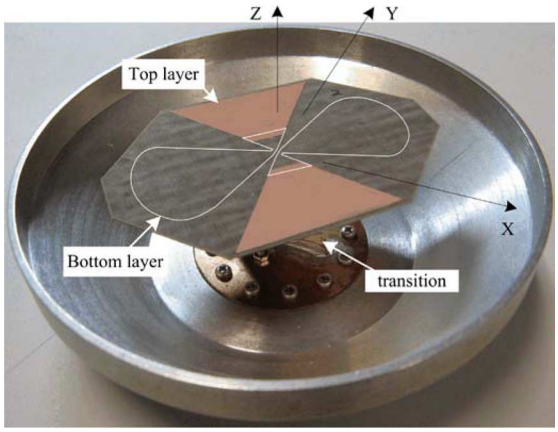

Fig. 4. Photograph of the fabricated antenna prototype.

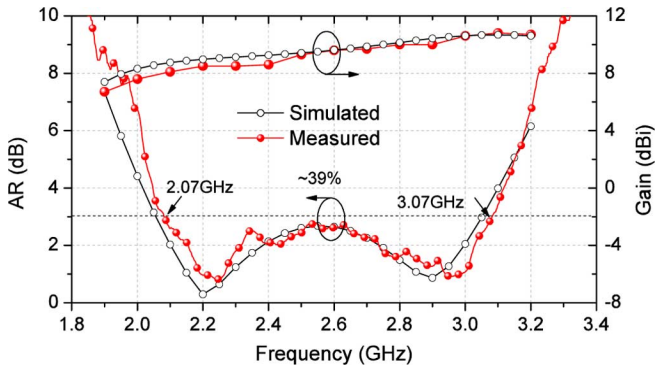

Fig. 5. Simulated and measured ARs and broadside gains.

of conical part of the cavity), $\alpha = 73°$ (flare angle of two bowtie dipoles), $R_C = 14$ (radius of round corners), $L_1 = 77.5$ ($0.664\lambda_0$, length of larger dipole), $L_2 = 51$ ($0.437\lambda_0$, length of small dipole), $L_3 = 13.35$ (position of loading gaps), $g = 1.2$ (size of loading gaps), $s = 0.4$, $w = 0.2$, $W_t = 25$ (width of transition), $l_s = 13$ (length of the DSL), $l_m = 6.54$ (length of the matching stripline), and $h_m = 24.54$ (height of the matching stripline), and the other detailed dimensions of the transition are given in Fig. 3 in mm. The total electrical dimensions of the proposed antenna are $1.028\lambda_0$ in diameter and $0.257\lambda_0$ in height.

III. Results and Analysis

A. Measured and Simulated Results

To verify our design, an antenna prototype with optimized dimensions was built, as shown in Fig. 4, and the measured and simulated ARs, broadside gains, and SWRs are shown in Figs. 5 and 6, respectively. Measurements agree reasonably well with simulations, and the whole measured frequency band for $\mathrm{AR} \leq 3$ dB is shifted slightly upwards over the simulated one. It can be seen that the proposed antenna presents a measured band of 2.07−3.07 GHz for $\mathrm{AR} \leq 3$ dB, corresponding to a fractional bandwidth of 39%, and in this frequency band the broadside gain is 8−10.7 dBi. It can be seen from Fig. 6 that the frequency band for $\mathrm{SWR} \leq 2$ ranges from 1.88 to over 3.4 GHz, covering the whole $\mathrm{AR} \leq 3$ dB frequency band and

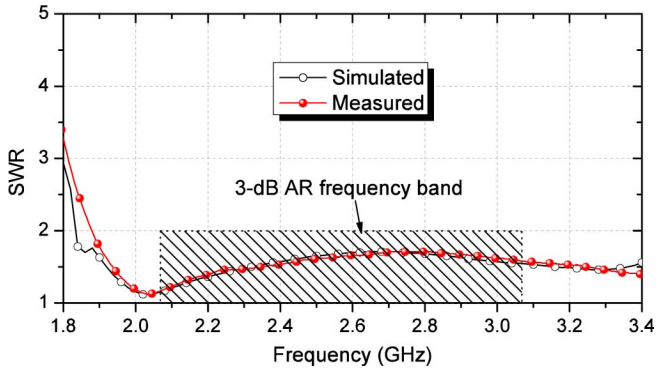

Fig. 6. Simulated and measured SWRs of the proposed antenna.

allowing the antenna operate in a circularly polarized manner with low reflection coefficient. The simulated and measured patterns in the XZ, YZ, and diagonal planes, at 2.2, 2.6, and 3 GHz respectively, are shown in Fig. 7, and measurements agree well with simulations along main beams. It can be seen that the antenna's main beam is fixed in the broadside direction and no side lobes appear in the whole frequency band. Although the cross-polarizations, i.e., left-hand circular polarized (LHCP) components, are sensitive to the fabrication errors and measurements, the measured results also agree reasonably well with the simulated ones. The antenna features good radiation patterns over the whole frequency band, such as large front-to-back ratio (FBR), symmetrical main beam, and small cross-polarization etc. The measured FBR is always over 25 dB, similar to the simulated 20 dB. It can also be observed from Fig. 7 that the antenna shows a very symmetrical right-hand circular polarized (RHCP) component and equal beam width in three planes.

B. Analysis of the Cavity-Backed Crossed TBA

To accurately design the proposed antenna for practical applications, its operating principles should be studied carefully. First of all, the conditions to produce good CP waves is very stringent for the proposed crossed dipoles topology in [12] and [13], where the input impedance relationships should be satisfied under the condition of no coupling between the two dipoles. For crossed wire dipoles, the coupling can be ignored due to their orthogonal electric field distributions. However, there is strong and complicated coupling between the arms of two bowtie dipoles, so the required relationships of input impedance are also altered compared with those proposed in [12]. It can be assumed that the input impedance Z can be formulated as $Z = R + jX$, where R is the input resistance and X is the input reactance, and the R-X diagram of our proposed antenna, as shown in Fig. 8, can clearly show this change of requirements to produce CP radiation [12], [13]. For example, at 2.2 GHz, the input resistances are 181.7 and 47.7 Ω, respectively, and the phase angle between them is $\ddot{\mathrm{O}}\Phi_1 = 81°$, and the phase angle is as small as $\Phi_2 = 28°$ at 2.5 GHz, and it can be even smaller as frequency increases, instead of 90° in [12] and [13].

For the cavity-backed antenna, its radiation is determined more directly by the electric field distribution in the aperture than by the current on the exciter. So a straightforward way to

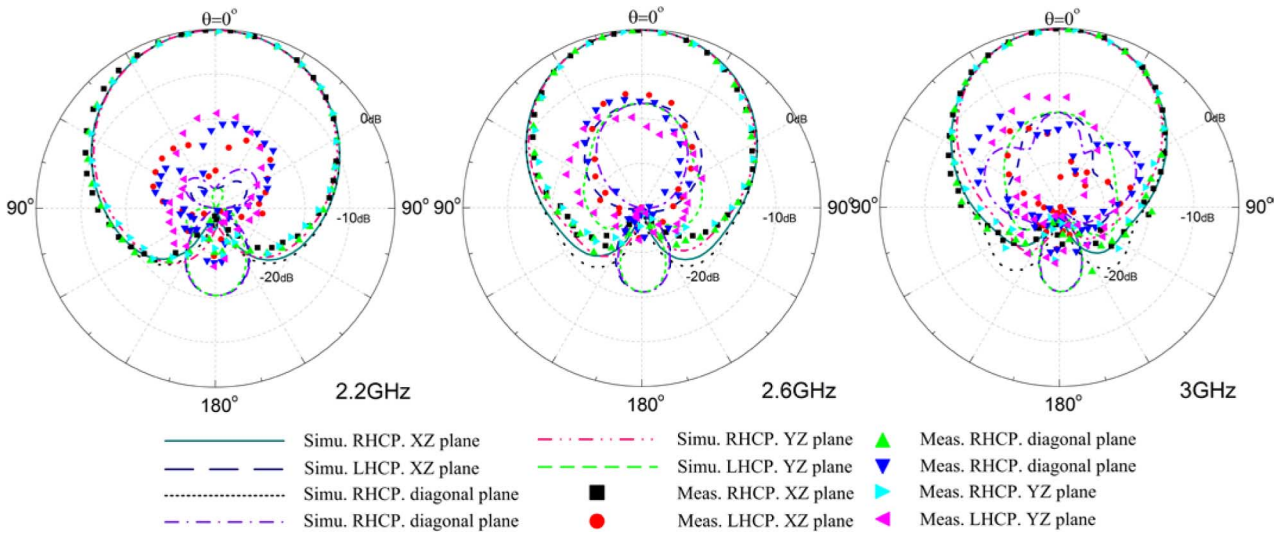

Fig. 7. Simulated and measured radiation patterns in XZ, diagonal, and YZ planes at 2.2, 2.6, and 3 GHz, respectively.

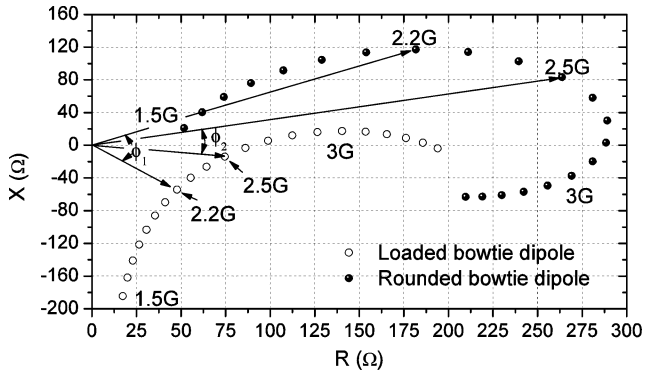

Fig. 8. R-X diagram of two bowtie dipoles of the exciter.

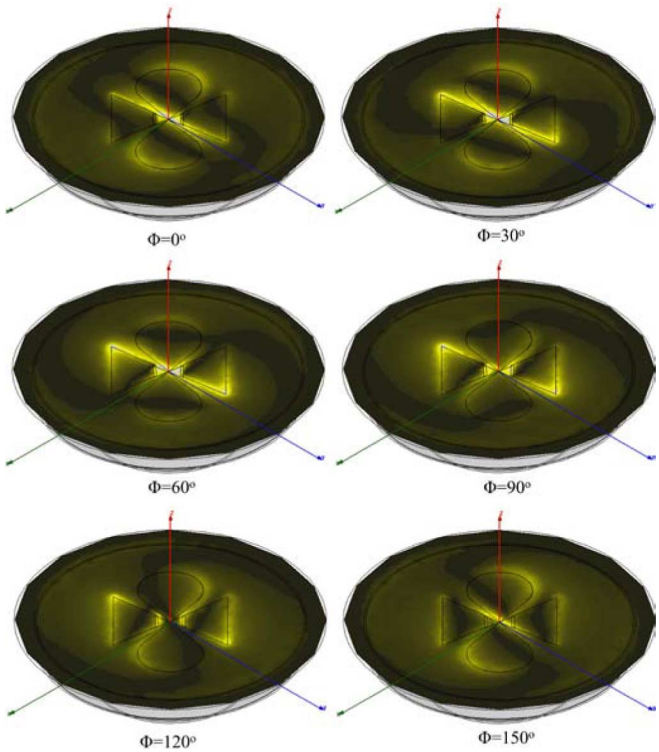

Fig. 9. Electric field distribution in the antenna aperture.

understand the CP behavior of our proposed antenna is to examine its electric field distribution in the aperture, as given in Fig. 9 with the phase angle $\Phi = 0°$, 30 °, 60°, 90°, 120°, and 150°, respectively. It can be seen that a right-hand rotated electric field is concentrated within the aperture and strong electric field between the edges of two dipoles proves strong coupling assumed above. It can be concluded that quite a different relationship of input impedances from the crossed thin-wire dipoles should be satisfied when there is strong coupling between the dipoles. Moreover, there is strong electric field near the sharp corners of the loaded dipole, which is why these corners cannot be rounded.

C. Issues About Transition

In this section, the functions of slots on the ground of transition are analyzed carefully. Fig. 10(a) gives the AR of the proposed antenna with different transitions. It can be seen that there is a resonance with poor AR shifted downwards from 2.43 to 2.12 GHz as the transition's width W_t increases from 10 to 20 mm (without slots), and this resonance will cause great reduction of the AR bandwidth. In order to move this resonance far away from the 3-dB AR frequency band, W_t is further increased and three pairs of slots are added at the same time because they can increase the length of current path, and finally the simulated resonance is shifted to 1.86 GHz, without any influence on AR bandwidth. Simulations prove that this phenomenon is caused by the resonance of transition. Fig. 10(b) gives the current distribution on one layer of the grounds of transition at 3 and 2.43 GHz, respectively. Ideally, the current should be concentrated very close to the signal line, e.g., the current at 3 GHz in Fig. 10(b). However, the large current density is also observed on the lower part of the ground, similar to a monopole shorted to the cavity's ground, thus the radiated linearly polarized waves

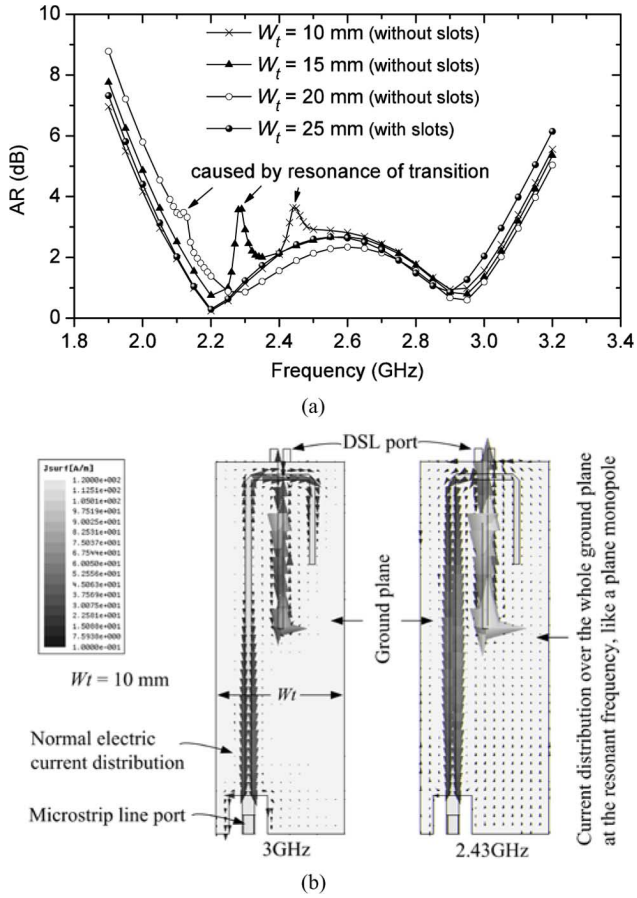

Fig. 10. Resonance of transition and its explanations. (a) AR versus different transitions. (b) Current distributions on the ground at 2.43 GHz and 3 GHz.

greatly deteriorate the CP performance at the resonance. Additionally, the air gap between the two layers of substrate dramatically influences the performances, which is one of main reasons causing differences between simulations and measurements.

IV. Parametric Studies and Discussions

To understand how the dimensions influence the antenna performances, parametric studies are performed by HFSS™. In this procedure, the feeding transition is also replaced by a 70 Ω lumped port to remove its influences on AR and to clearly show the change of the antenna's input impedance. When one parameter is studied, the others are kept identical to their optimized values. In the parametric studies, the AR as well as input impedance is emphasized, and the broadside gain is almost immune to the parameters of the exciter.

The first issue focused is the gap width g and its position L_3 related to the capacitive loading on the exciter. As shown in Fig. 11, when the loaded gaps are placed with a small distance, i.e., L_3 is small, the AR bandwidth will be reduced and the center frequency will be shifted upward at the same time. However, the circular polarization will be deteriorated as L_3 becomes too large because the input resistance and input reactance of the capacitive loaded bowtie dipole will be changed simultaneously. For the input impedance in Fig. 12, small L_3 leads to large input resistance as well as large input reactance, and large

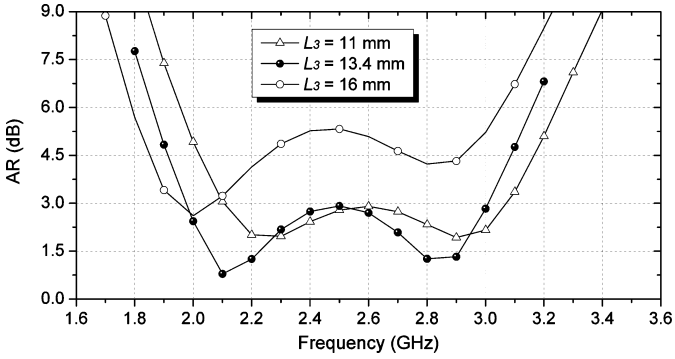

Fig. 11. AR of antenna with different gap position L_3.

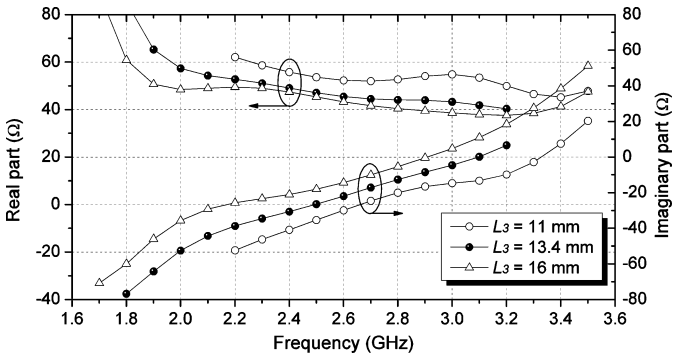

Fig. 12. Input impedance of antenna with different gap position L_3.

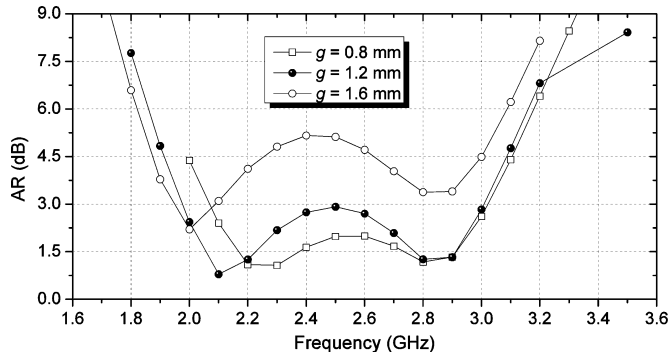

Fig. 13. AR of the antenna with different gap size g.

input resistance is of benefit for matching, but large input reactance makes the good impedance matching difficult. So, an appropriate value of L_3 should be chosen for a better AR and easy matching.

The gap width g is another critical parameter, and it can be seen from Fig. 13 that the AR is very sensitive to g. A smaller g causes better in-band AR but narrower 3-dB AR bandwidth, and obviously the largest 3-dB AR bandwidth can be achieved as $g = 1.2$ mm. From Fig. 14, the gap width g influences input reactance more than input resistance because g determines the value of capacitive loading of the smaller bowtie dipole.

The total size L_2 of capacitively loaded bowtie dipole is also a critical parameter that it does not change the second minimum point of the AR but obviously shift the first one at the cost of worse in-band AR as shown in Fig. 15. Thus, an appropriate value of $L_2 = 51$ mm can bring largest bandwidth, and also

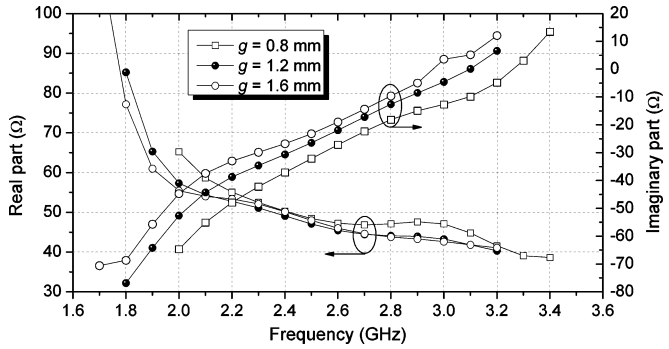

Fig. 14. Input impedance of the antenna with different gap size g.

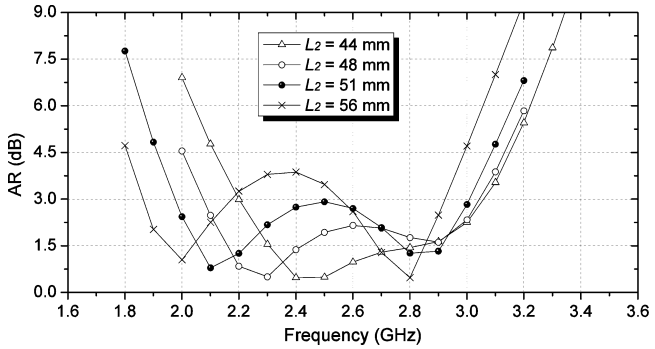

Fig. 15. AR of the antenna with different L_2.

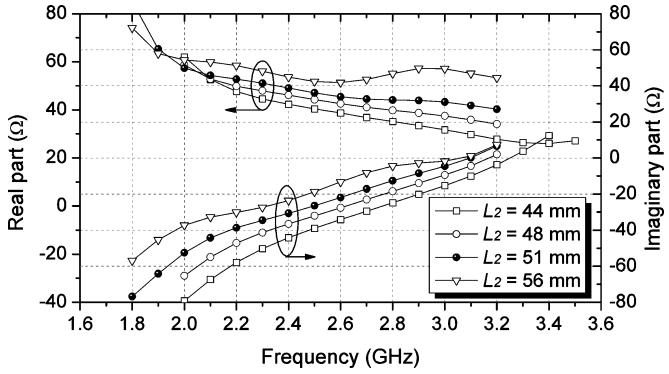

Fig. 16. Input impedance of the antenna with different L_2.

larger L_2 causes flatter and larger input resistance and smaller input reactance as shown in Fig. 16, which are both of benefit for good impedance matching.

The larger rounded bowtie dipole is determined by three parameters: total length L_1, the flare angle α, and radius R_C of round corners. Actually they are relative to each other. According to our previous investigations [18], the largest R_C is of benefit to achieve the best performance, and in this case the two arcs are connected to one part of an inscribed circle of the triangular bowtie dipole. Thus, a formula can be given to describe their relationships

$$R_C = \frac{L_1 \sin\left(\frac{\alpha}{2}\right)}{2 + 2\sin\left(\frac{\alpha}{2}\right)}. \tag{1}$$

But here they are still studied individually in order to clearly show their influences on antenna performance.

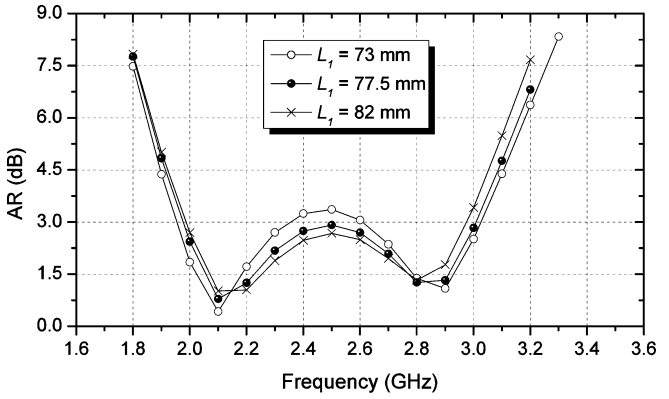

Fig. 17. AR of the antenna with different size L_1 of rounded bowtie dipole.

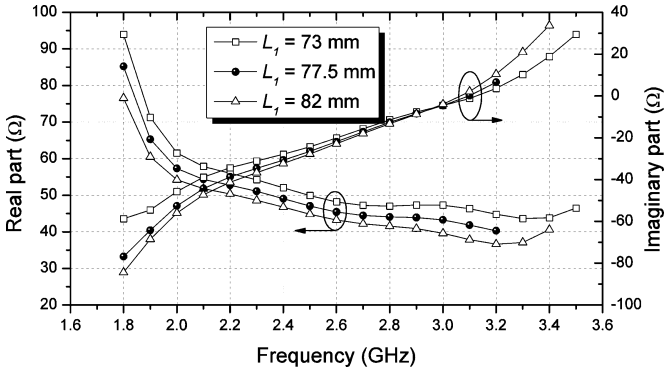

Fig. 18. Input impedance of the antenna with different L_1.

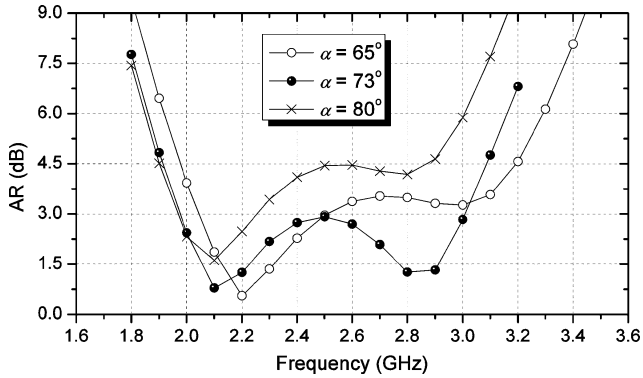

Fig. 19. AR of the antenna with different α.

From Figs. 17 and 18, it can be seen that L_1 mainly influences input resistance of the antenna, and a smaller L_1 causes slightly larger AR bandwidth but worse in-band AR, while a larger one produces smaller AR bandwidth but better in-band AR. Thus, a suitable L_1 should be selected according to the expected AR in-band. The flare angle α has definitely influences on both AR and input impedance, as shown in Figs. 19 and 20. It can be observed that the second minimum AR point almost disappears as α is changed far from 73°. The final parameter studied is R_C, as given in Figs. 21 and 22. When R_C is small, the second AR minimum point is superposed with the first one, and it is shifted upwards as R_C is increased from 8 to 14 mm, so the AR bandwidth is also increased versus R_C. Moreover, a large R_C can also bring both the flattest input resistance and input reactance, which makes impedance matching more easily.

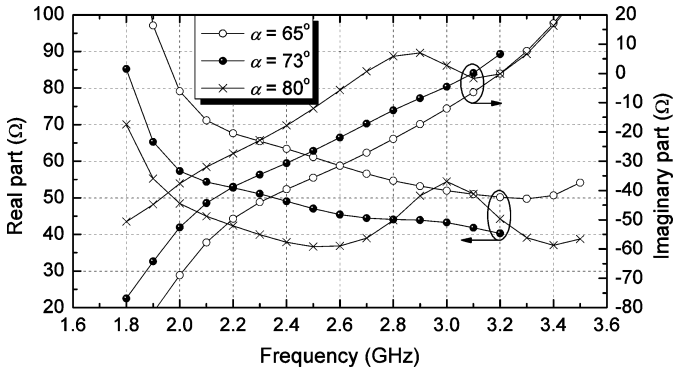

Fig. 20. Input impedance of the antenna with different α.

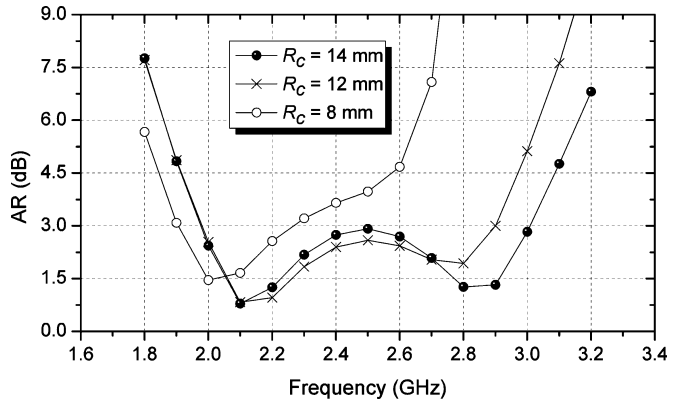

Fig. 21. AR of the antenna with different R_C.

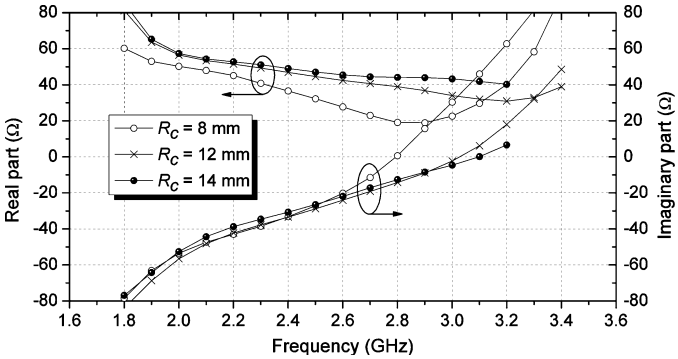

Fig. 22. Input impedance of the antenna with different R_C.

V. Conclusion

A composite cavity-backed CBD is investigated in the paper. Good results and good agreement between simulations and measurements prove the success of the proposed antenna as a candidate for wideband CP applications. Operating principles of the proposed antenna, as given in the paper, is quite different from the crossed thin-wire dipoles because of strong coupling between the two bowtie dipoles. After successful relocating the resonance of the transition downwards, the antenna presents the largest 3-dB AR bandwidth of 39.2%, impedance bandwidth of 57.6% for SWR $\leq$ 2, and symmetrical radiation patterns. Referencing the given design procedure, final results, and parametric studies, it will not be time consuming to design this antenna at the interesting frequencies, although it did take us much time to find the optimized solution, especially the resonance phenomenon of the feeding transition.

References

[1] K.-L. Lau, K.-M. Luk, and K.-F. Lee, "Design of a circularly-polarized vertical patch antenna," *IEEE Trans. Antennas Propag.*, vol. 54, pp. 1332–1335, Apr. 2006.

[2] K.-F. Tong and J. Huang, "New proximity coupled feeding method for reconfigurable circularly polarized microstrip ring antennas," *IEEE Trans. Antennas Propag.*, vol. 56, pp. 1860–1866, Jul. 2008.

[3] J. R. James and P. S. Hall, *Handbook of Microstrip Antennas*. London, U.K.: Peter Peregrinus, 1989, ch. 4.

[4] K. L. Lau and K. M. Luk, "Novel wide-band circularly polarized patch antenna based on L-probe and aperture-coupling techniques," *IEEE Trans. Antennas Propag.*, vol. 53, pp. 577–580, Jan. 2005.

[5] K. L. Lau and K. M. Luk, "A wide-band circularly polarized L-probe coupled patch antenna for dual-band operation," *IEEE Trans. Antennas Propag.*, vol. 53, pp. 2636–2644, Aug. 2005.

[6] J.-M. Laheurte, "Dual-frequency circularly polarized antennas based on stacked monofilar square spirals," *IEEE Trans. Antennas Propag.*, vol. 51, pp. 488–492, Mar. 2003.

[7] W. K. Lo, C. H. Chan, and K. M. Luk, "Circularly polarized microstrip antenna array using proximity coupled feed," *Eletron. Lett.*, vol. 34, no. 23, pp. 2190–2191, Nov. 1998.

[8] J.-W. Baik, K.-J. Lee, W.-S. Yoon, T.-H. Lee, and Y.-S. Kim, "Circularly polarised printed crossed dipole antennas with broadband axial ratio," *Electron. Lett.*, vol. 44, no. 13, pp. 785–786, Jun. 2008.

[9] R. K. Zimmerman, jr, "Crossed dipoles fed with a turnstile network," *IEEE Trans. Microw. Theory Tech.*, vol. 46, no. 12, pp. 2151–2156, Dec. 1998.

[10] J. L. Wong and H. E. King, "A cavity-backed dipole antenna with wide-bandwidth characteristics," *IEEE Trans. Antennas Propag.*, vol. 21, pp. 725–727, Sep. 1973.

[11] S. Ohmori, S. Miura, K. Kameyama, and H. Yoshimura, "An improvement in electrical characteristics of a short backfire antenna," *IEEE Trans. Antenna Propag.*, vol. AP-31, no. 4, pp. 644–646, Jul. 1983.

[12] M. F. Bolster, "A new type of circular polarizer using crossed dipoles," *IRE Trans. Microw. Theory Tech.*, vol. 9, no. 5, pp. 385–388, Sep. 1961.

[13] R. Li, D. C. Thompson, J. Papapolymerou, J. Laskar, and M. M. Tentzeris, "A circularly polarized short backfire antenna excited by an unbalance-fed cross aperture," *IEEE Trans. Antennas Propag.*, vol. 54, pp. 852–859, Mar. 2003.

[14] K.-L. Lau, H. Wong, and K.-M. Luk, "A full-wavelength circularly polarized slot antenna," *IEEE Trans. Antennas Propag.*, vol. 54, pp. 741–743, Feb. 2006.

[15] Y. Kazama, "One-point feed printed crossed dipole with a reflector antenna combined with a reactively loaded parasitic loop for land mobile satellite communication antennas," *IEE Proc. -H*, vol. 140, no. 5, pp. 417–420, Oct. 1993.

[16] S.-W. Qu, J.-L Li, Q. Xue, C. H. Chan, and S. Li, "Wideband and unidirectional cavity-backed folded triangular bowtie antenna," *IEEE Trans. Antennas Propag.*, vol. 57, pp. 1259–1263, Apr. 2009.

[17] S.-W. Qu, C. H. Chan, and Q. Xue, "Ultrawideband composite cavity-backed folded sectorial bowtie antenna with stable pattern and high gain," *IEEE Trans. Antennas Propag.*, vol. 57, pp. 2478–2483, Aug. 2009.

[18] S.-W. Qu, C. H. Chan, and Q. Xue, "Ultrawideband composite cavity-backed rounded triangular bowtie antenna with stable patterns," *J. of Electromagn. Waves Applicat.*, vol. 23, pp. 685–695, 2009.

[19] S.-W. Qu, J.-L. Li, Q. Xue, and C. H. Chan, "Wideband cavity-backed bowtie antenna with pattern improvement," *IEEE Trans. Antennas Propag.*, vol. 56, pp. 3850–3854, Dec. 2008.

[20] Q. Xue, S.-W. Qu, and C. H. Chan, "Wideband cavity-backed bowtie antennas," in *2009 IEEE International Workshop on Antenna Technology on Small Antennas and Novel Metamaterials (iWAT2009)*, Santa Monica, California, Mar. 2009, pp. 1–4.

[21] A. Kumar and H. D. Hristov, *Microwave Cavity Antennas*. Norwood, MA: Artech House, 1989.

[22] R. Li, G. DeJean, J. Laskar, and M. M. Tentzeris, "Investigation of circularly polarized loop antennas with a parasitic element for bandwidth enhancement," *IEEE Trans. Antennas Propag.*, vol. 53, pp. 3930–3939, Dec. 2005.

[23] "HFSS: High Frequency Structure Simulator Based on the Finite Element Method," Ansoft Corp.

Shi-Wei Qu was born in He'nan province, China, in October, 1980. He received the B.Eng. and M.Sci. degrees from the University of Electronic Science and Technology of China (UESTC), Chengdu, in 2001 and 2006, respectively, and the Ph.D. degree in the City University of Hong Kong (CityU), in October 2009.

He is currently a COE (Global Center of Excellence) Fellow and a Postdoctoral Fellow in Tohoku University, Sendai, Japan. From 2001 to 2002, he worked for the 10th Institute of Chinese Information Industry. From 2006 to 2007, he was a Research Assistant in the Department of Electronic Engineering, City University of Hong Kong. His research interests include UWB antennas and arrays, metamaterial applications in antennas, and millimeter-wave antennas and arrays, etc.

Chi Hou Chan (S'86–M'86–SM'00–F'02) received the Ph.D. degree in electrical engineering from the University of Illinois at Urbana-Champaign, in 1987.

He joined the Department of Electronic Engineering, City University of Hong Kong, China, in 1996 and was promoted to Chair Professor of Electronic Engineering in 1998. From 1998 to 2009, he was first Associate Dean then Dean of College of Science and Engineering. He has been Acting Provost of the university since July 2009. His research interests cover computational electromagnetics, antennas, microwave and millimeter-wave components and systems, and RFICs.

Prof. Chan received the US National Science Foundation Presidential Young Investigator Award in 1991 and the Joint Research Fund for Hong Kong and Macau Young Scholars, National Science Fund for Distinguished Young Scholars, China, in 2004. For teaching, he received the outstanding teacher awards in EE Department at CityU in 1998, 1999, 2000 and 2008. Students he supervised also received numerous awards including the Third (2003) and First (2004) Prizes in the IEEE International Microwave Symposium Student Paper Contests, the IEEE Microwave Theory and Techniques Graduate Fellowship for 2004–2005, Undergraduate/Pre-Graduate Scholarships for 2006–2007 and 2007–2008, and the 2007 International Fulbright Science and Technology Fellowship offered by the US Department of State.

Quan Xue (M'02–SM'04) received the B.S., M.S., and Ph.D. degrees in electronic engineering from the University of Electronic Science and Technology of China (UESTC), Chengdu, in 1988, 1990, and 1993, respectively.

In 1993, he joined the UESTC as a Lecturer. He became an Associate Professor in 1995 and a Professor in 1997. From October 1997 to October 1998, he was a Research Associate and then a Research Fellow with the Chinese University of Hong Kong. In 1999, he joined the City University of Hong Kong, where he is currently an Associate professor in the Department of Electronic Engineering. He serves as the Deputy Director of State Key Laboratory (Hong Kong) of Millimeter-waves of China. He has authored or coauthored over 160 internationally referred papers and over 60 international conference papers. His current research interests include microwave passive components, active components, antenna, microwave monolithic integrated circuits (MMIC), and radio frequency integrated circuits (RFIC).

Dr. Xue was awarded the UESTC "distinguished academic staff" for his contribution to the development of millimeter-wave components and subsystems. He is the Region 10 Coordinator of IEEE MTT-S AdCom.